J Inorg Organomet Polym (2015) 25:702–711
DOI 10.1007/s10904-014-0148-3

Synthesis and Structure Characterizations of Coordination Polymers Based on Silver(I) and Nitrogen Donors

Safaa El-din H. Etaiw · Mohamed M. El-bendary · Abd El-Aziz S. Fouda · Manal Maher

Received: 14 November 2014 / Accepted: 10 December 2014 / Published online: 18 December 2014

Abstract Yellow crystals of the coordination polymers (CP) [Ag(qox)NO_3], **1** [Ag(pyzca)], **2** were obtained by the reaction of $AgNO_3$, quinoxaline (qox) or pyrazinecarboxylic acid (pyzcaH), respectively. The crystal structure of **1** displays 1D-extended chain of $[Ag(qox)]_n$ with NO_3 coordinated to every Ag atom. The 1D-chains of **1** are interconnected by strong hydrogen bonds, π–π stacking and short contacts developing two dimensional sheets containing channels. Furthermore, the overall packing arrangement of **1** results 3D topology with corrugated network. The Ag atom in **2** acquires tetrahedral geometry while each pyzca ligand provides three donor sites connected to three Ag atoms. The structure of CP **2** displays 1D-extended helical chain of $[Ag(pyzca)]_n$. The 3D-packing of the CP **2** creates nanometer pores. The luminescence properties of **1** and **2** were discussed.

Keywords Silver coordination polymers · Quinoxaline · Pyrazinecarboxylic · Luminescence properties

1 Introduction

Crystal design and engineering of coordination polymers (CP) have been the focus of intense research efforts around the world, in part because of not only their unique structural motifs, but also for their numerous potential applications in catalysis, gas storage, optics fluorescence, magnetism, corrosion inhibitions and antitumor activity [1–14]. The selection of the metal ions and ligand is extremely important in the construction and the design of the CP [15]. Among the ligands, N-containing heterocyclic derivatives are excellent neutral ligands to generate the interesting architectures with metal ions. Meanwhile, pyrazine and its derivative have been used as the building blocks to obtain a variety of CP [16–22]. Pyrazine carboxylic and quinoxaline are good candidates for molecular building blocks because of their rod like rigidity and length. Also, the flexible coordination geometries of Ag(I) cation contributes significantly to the different structural topologies and dimensionalities of Ag(I) CP. In addition, H-bonding, Ag···π, π···π stacking, and host–guest interactions also affect the results, and they may further link discrete subunits or low-dimensional entities into high-dimensional networks [23–28]. Furthermore, the closed shell d^{10} electronic configuration of Ag(I) results in argentophilic interactions, which play an important role in constructing fascinating structures [29–33]. In the previous literature, many Ag(I) CP based on pyrazine, quinoxaline and their derivatives have been obtained, however complicated silver units in these CP were seldom observed [34–41]. Based on the above considerations, our interest has been focused on pyrazine-2-carboxylate and quinoxaline ligands silver CP.

Here we report the synthesis, structural characterization and luminescence of the CP [Ag(qox)NO_3], **1** and [Ag(pyzca)], **2**, from the simple reactions of $AgNO_3$ and

Electronic supplementary material The online version of this article (doi:10.1007/s10904-014-0148-3) contains supplementary material, which is available to authorized users.

S. E. H. Etaiw (✉) · M. M. El-bendary · M. Maher
Chemistry Department, Faculty of Science, Tanta University, Tanta, Egypt
e-mail: safaaetaiw@hotmail.com

A. E.-A. S. Fouda
Department of Chemistry, Faculty of Science, El-Mansoura University, El-Mansoura 35516, Egypt

the quinoxaline (qox) or pyrazinecarboxylic acid (pyzcaH), in H_2O/acetonitrile/NH_3 media at room temperature. Further, we report on the crystal packing effects, namely H-bonds, and π–π stacking interactions, metal–ligand, which may have an effect on the formation and stability of **1**, **2**. Also, among the various aspects of chemical sciences concerned with qox and pyzca, we focus on their versatility to afford a luminescent material at room temperature. Curiously, unmodified qox and pyzca are weakly emissive compounds, but on complexation with silver a highly luminescent complex should be obtained to be used as luminescent probe.

2 Experimental

2.1 Materials and Physical Measurements

All chemicals and solvents used in this study were of analytical grade supplied by Aldrich or Merck and used as received. The Infrared (IR) spectra were recorded on Perkin Elmer 1430 Ratio Recording Infrared Spectrophotometer as KBr discs. Thermogravimetric analysis was carried out on a Shimadzu AT 50 thermal analyzer (under N_2 atmosphere). Electronic absorption spectra as solid matrices and in DMF were measured on Shimadzu (UV-3101 PC) spectrometer. Fluorescent spectra as solid matrices and in DMF were measured with a Perkin Elmer (LS 50 B) spectrometer.

2.2 Syntheses of [Ag(qox)(NO_3)], **1** and [Ag(pyzca)], **2**

A solution of 0.08 g (0.5 mmol) of $AgNO_3$ in 20 mL of H_2O was added dropwise with stirring, to a solution containing 0.077 g (0.5 mmol) of quinoxaline (qox) in 15 mL acetonitrile. A white precipitate was formed, ammonia solution was added to obtain a clear solution. Already after 2 weeks a yellow needle crystals were resulted from clear solution, after filtration, subsequent washing with water and overnight drying, about 50 mg (45.2 % referred to $AgNO_3$) of yellow crystals were obtained. Anal. Calc. C, 32.02; H, 2.02; N, 14.0 %. Found: C, 32.11; H, 1.92; N, 14.02 %.

For **2**, a solution of 0.08 g (0.5 mmol) of $AgNO_3$ in 20 mL of H_2O was added dropwise with stirring, to a solution of 0.062 g (0.5 mmol) of pyrazinecarboxylic acid (pyzcaH) in 30 mL acetonitrile. A white precipitate was formed, ammonia solution was added to obtain a clear solution. Already after 2 weeks a yellow prismatic crystals were resulted, after filtration, subsequent washing with water and overnight drying, about 55 mg (45.2 % referred to $AgNO_3$) of yellow crystals were obtained. Anal. Calc. C, 26.0; H, 1.31; N, 12.13 %. Found: C, 25.91; H, 1.22; N, 12.32 %.

2.3 Crystal Structure Determination

Structural measurements for **1** and **2** were performed on a Kappa CCD Enraf–Nonius FR 90 four circle goniometer with graphite monochromatic MoKα radiation {[λMoKα] = 0.71073 Å} at 25 ± 2 °C. The structures were resolved using direct-methods and all of the non-hydrogen atoms were located from the initial solution or from subsequent electron density difference maps during the initial stages of the refinement. After locating all of the non-hydrogen atoms in each structure the models were refined against F^2, first using isotropic and finally using anisotropic thermal displacement parameters. The positions of the hydrogen atoms were then calculated and refined isotropically, and the final cycle of refinements was performed. Crystallographic data for **1** and **2** are summarized in Table 1.

3 Results and Discussion

3.1 Crystal Structure of [Ag(qox)NO_3], **1**

Single crystal X-ray analysis reveals that **1** crystallizes in the orthorhombic space group $P2_12_12_1$ and the asymmetric

Table 1 Crystal data for the CP **1** and **2**

	1	**2**
Empirical formula	$C_8H_6AgN_3O_3$	$C_5H_3AgN_2O_2$
Formula weight g/mol	300.014	230.961
Temperature (K)	298	298
Crystal system	Orthorhombic	Orthorhombic
Space group	$P2_12_12_1$	$Pna2_1$
a/Å	7.3213 (5)	7.0443 (3)
b/Å	9.1822 (6)	11.5211 (5)
c/Å	13.1781 (11)	6.9549 (3)
α/°	90.00	90.00
β/°	90.00	90.00
γ/°	90.00	90.00
V/Å^3	885.91 (11)	564.45 (4)
Z	4	4
μ(Mo-Kα)/m m^{-1}	2.26	3.49
Calculated density/mg cm^{-3}	2.250	2.718
Goodness-of-fit on F^2	1.066	1.006
F(000)	584	440
R indices[$I > 3\sigma(I)$] R_1/wR_2	0.032/0.088	0.027/0.084
R indices(all data)	0.056/0.094	0.038/0.086
R_{int}	0.043	0.021
Data/restraints/parameters	843/0/136	711/0/91

unit consists of one silver atom, one qox molecule and one nitrate molecule, Fig. 1a. The structure of the CP **1** consists of 1D-extended chain of $[Ag(qox)]_n$ with NO_3 coordinated to every Ag atom. Each Ag(I) center is coordinated to two nitrogen atoms from different but crystallographically identical qox ligands to form a distorted linear chain of alternating Ag(I) and qox, Fig. 1b. Ag–N bond distances are in the range of 2.257–2.292 Å, which are typical values for Ag(I)–N_{py} coordination distances [39, 42–48]. N6–Ag1–N7 bond angle of 164.42° is indicative of the presence of a distortion from linearity in the structure of **1**, which may be ascribed to the strong interaction between Ag(I) and an adjacent nitrate molecule; Ag1–O4 = 2.607 Å. Thus, the coordination environment around Ag(I) can be also described as a distorted T-shaped coordination geometry due to the semi-coordinative interaction between Ag1 and oxygen of the nitrate molecule causing pyramidization of the silver atom in such a way that the angles of the planar trigonal geometry around the silver sites deviate largely than 120° (Table 2). In addition, short contacts between silver atom in one molecule and the nitrate group in adjacent one (Ag1–N2 = 3.21 and Ag1–O4 = 2.739 Å) cause pyramidization of the silver atom (Table 2).

The 1D-chains are interconnected by strong hydrogen bonds between the oxygen of the nitrate group in one chain and the hydrogen atoms of the qox ligand in another chain O19–H20 = 2.528 Å, O13–H9 = 2.824 Å, developing two dimensional sheets (Table 3; Fig. 2). There is also π–π stacking between the parallel chains between oxygen atoms of nitrate in one chain and carbon atoms of qox in another chain (O13–C11 = 3.370 Å, O13–C20 = 3.296 Å and O4–C8 = 3.320 Å). Indeed, self-assembly by coordination bonds, hydrogen bonds, π–π stacking and short contacts between silver atom in one chain and the carbon atom of the qox in another chain (Ag1–C20 = 3.407 Å) grow the structure of **1** to a three dimensional network (Fig. 3; Table 2). The packing of the CP **1** creates channels with the Ag···Ag separation distance between the adjacent layers of $[Ag\mu_2(qox)]_n$ equals to 7.745 Å. These channels accommodate the coordinated nitrate ions (Figs. 3, 4). Comparing the structure of **1** with that of $[Ag(quinoxaline)]_n(NO_3)_n]$, **1′** [39] reveals that the crystal packing of the chains in **1′** is characterized by a pairwise association of parallel chains separated by stacks of nitrate ions. There is no π-stacking between the parallel chains because the chains are displaced such that the aromatic groups

Table 2 Bond lengths (Å) and bond angles (°) of the CP **1**

Ag1–O4	2.607 (4)	N6–Ag1–O13	92.0 (4)
Ag1–O4^{i}	2.739 (4)	N6–Ag1–O19^{i}	95.4 (3)
Ag1–N6	2.257 (6)	N7–Ag1–O13	86.1 (4)
Ag1–N7	2.292 (6)	N7–Ag1–O19^{i}	98.5 (3)
Ag1–O13	2.942 (5)	O13–Ag1–O19^{i}	124.06 (12)
Ag1–O19^{i}	2.829 (7)	O4–N2–O13	119.4 (5)
N2–O4	1.243 (7)	N6–Ag1–N7	164.42 (14)
N2–O19	1.238 (7)	O4–N2–O13	119.4 (5)
C11–O13	3.370 (7)	O4–N2–O19	118.9 (6)
C20–O13	3.296 (7)	O13–N2–O19	121.6 (7)
C8–O4	3.320 (7)	O4–N2–O13	119.4 (5)
Ag1–C20	3.407 (4)	O4–N2–O19	118.9 (6)
Ag1–Ag1^{i}	5.1999 (4)	Ag1–O2–N2	106.10 (7)

Symmetry codes: (i) −x, 1/2 + y, 3/2 − z

Table 3 Hydrogen bond lengths (Å) and bond angles (°) in the CP **1**

D–H···A	d (D–H)	d (H···A)	d (D···A)	∧ (DHA)
C20–H20···O19	0.960	2.528	3.155	122.99
C21–H21···O19	0.960	2.470	3.157	127.60
C8–H8···O4	0.960	2.680	3.320	124.56
C11–H11···O19	0.960	2.539	3.207	126.72
C9–H9···O13	0.960	2.824	3.161	101.67
C20–H20···O13	0.960	2.772	3.155	123.99
C8–H8···O19	0.960	2.759	3.220	122.536
C12–H12···O4	0.960	2.765	3.133	127.23
C21–H21···O4	0.960	2.795	3.120	120.85
C9–H9···O4	0.960	2.680	3.230	104.56
C12–H12···O13	0.960	3.082	3.199	88.16

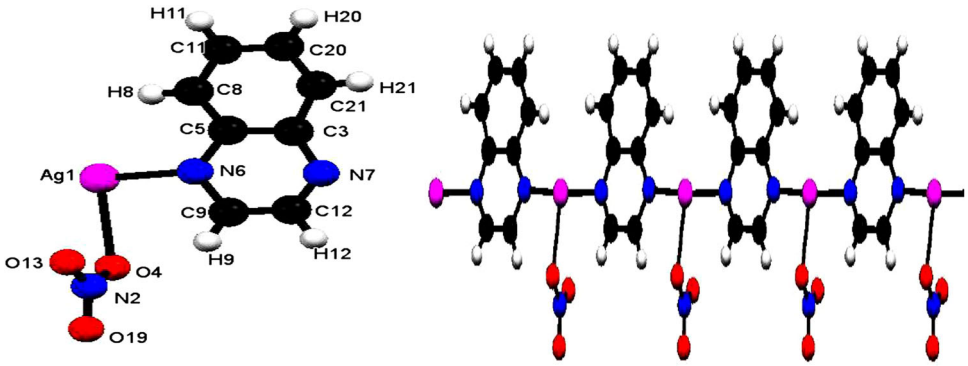

Fig. 1 An ORTEP plot of the asymmetric unit of the CP **1** with atom labeling scheme (**a**); repeated unit of the CP **1** giving 1D-chain (**b**)

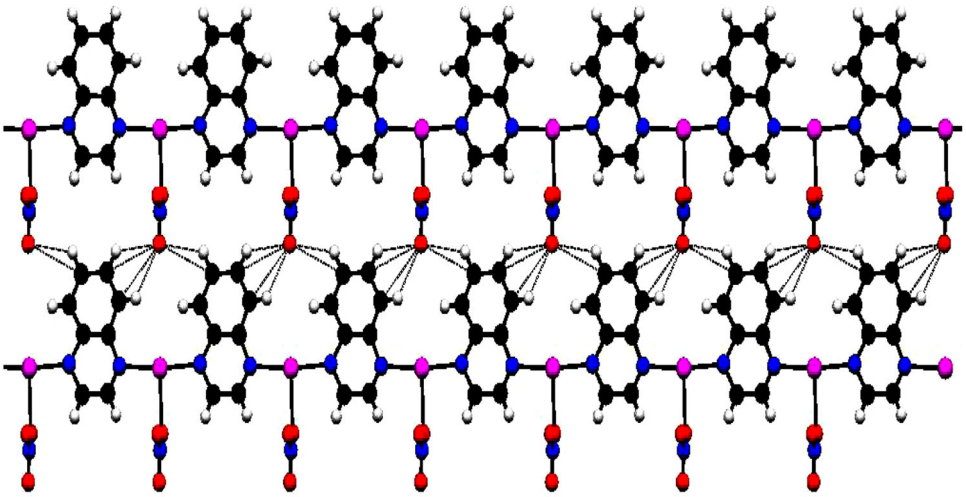

Fig. 2 2D-sheet of the CP **1** via H-bonds along the *b* axis

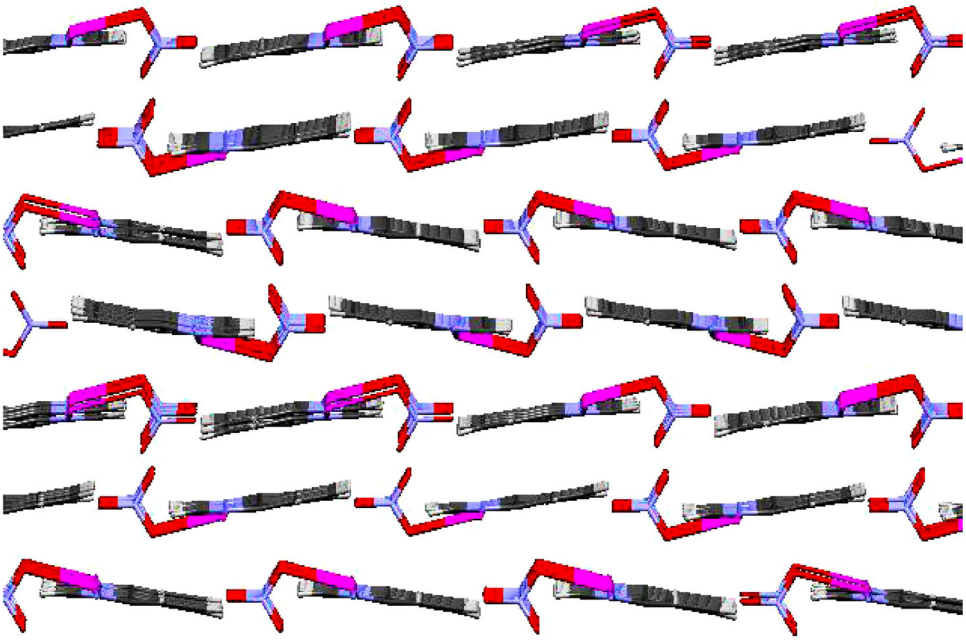

Fig. 3 3D-network with channels of **1** along the *a* axis

do not face each other but instead face the silver ions from the neighboring chain, although without any significant Ag···C or Ag···H interactions and the nitrates are clearly separated from these units which is not the case in **1**. In the structure of **1,** hydrogen bonds, π–π stacking and short contacts represent the essential role to develop 3D- network.

3.2 Crystal Structure of [Ag (pyzca)], **2**

The asymmetric unit of the CP **2** consists of one silver atom and one pyzca molecule, Fig. 5a. Each Ag atom is four-coordinated with two carboxylate oxygen atoms and two nitrogen atoms from different but crystallographically identical pyzca ligands creating a five chelate ring; C6C8O2Ag1N4 (Fig. 5b). The distances of N4–Ag1, N3–Ag1, $O2^{i}$–Ag1 and Ag1–O2 are 2.333 (3), 2.229 (3), 2.324 (3) and 2.548 (3) Å, respectively. It is noticed that the Ag–O distances are different and the elongation of the Ag1–O2 causes the formation of a distorted tetrahedral structure. The angles of the tetrahedral are N3–Ag–O2 = 127.51 (2)°, N4–Ag–$O2^{i}$ = 91.07 (11)°, $O2^{i}$–Ag–N3 = 101.41 (12)° and O2–Ag–N4 = 67.38 (9)° (Table 4). These angles deviate largely than being 109° due to the pyramidization of the tetrahedral structure around the silver atoms which is also caused by close Ag–C and Ag–O contacts; Ag1–C11 = 3.083 (9) Å, Ag1–C7 = 3.159 (11) Å and Ag1–O2 = 2.548 (9) Å (Table 5). Each pyzca ligand provides three donor sites connected to three Ag atoms.

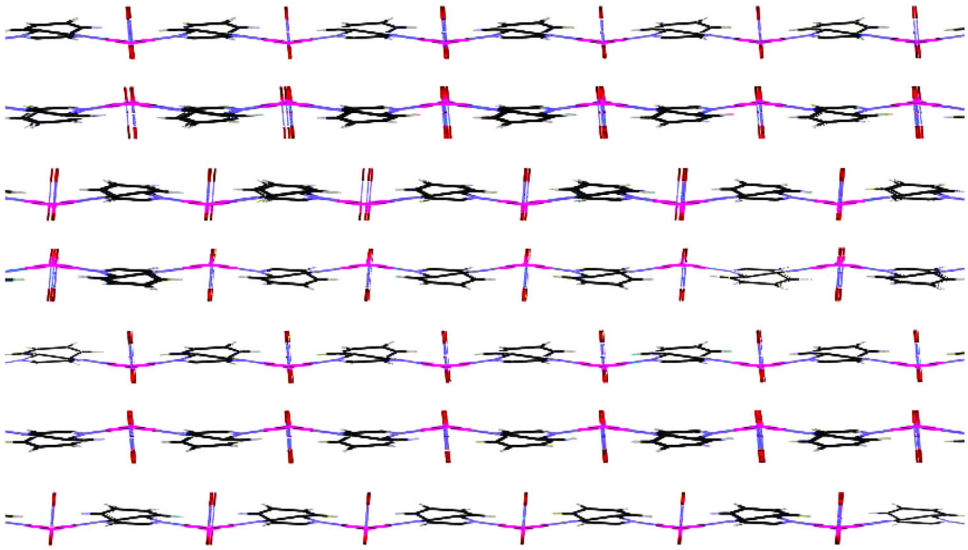

Fig. 4 3D-network with channels of **1** along the *b* axis

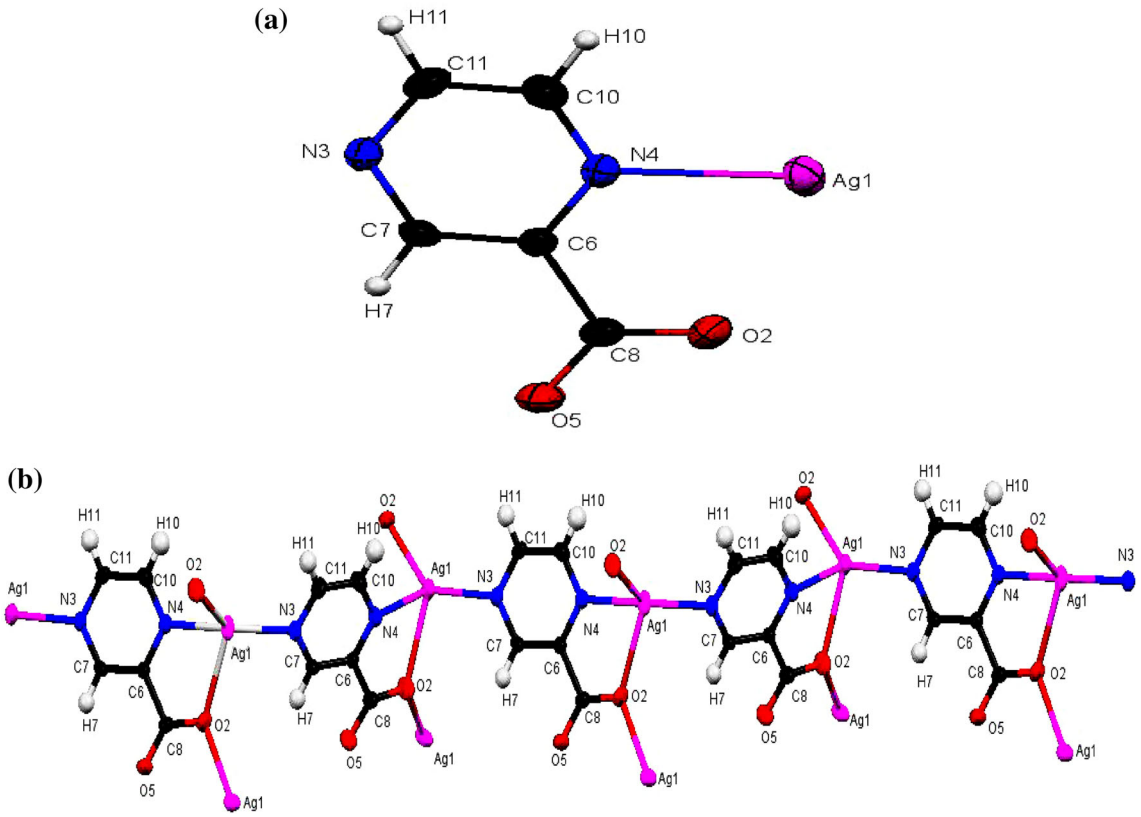

Fig. 5 An ORTEP plot of the asymmetric unit of the CP **2** (**a**). Expanded structure of the CP **2** showing the pentagonal ring of C6C8O2Ag1N4 and the helical structure along the *a* axis with atom labeling scheme (**b**)

Alternatively, single crystal X-ray analysis reveals that the CP **2** displays 1D-extended helical chain of $[Ag(pyzca)]_n$. The one-dimensional helical chain running along the a-axis with a pitch of 7.123 (8) Å (Fig. 5b). The Ag–N–C angle in the helical Ag(pyzca) chain is 117.781°. The intra-chain adjacent Ag···Ag distances is 4.272(4) Å. The pyzca ligand in **2** acts as a bridging group where each nitrogen atom of pyrazine moiety coordinates to silver(I) ion, and one oxygen of the carboxylate group (O2) also bridges to two silver atoms while O5 is free. The 1D-chains are interconnected

Table 4 Bond lengths (Å) and bond angles (°) of the CP **2**

Ag1–O2	2.548 (3)	O2–Ag1–O2^{i}	118.87 (4)
Ag1–O2^{i}	2.324 (3)	O2–Ag1–N3^{ii}	101.41 (12)
Ag1–N3^{ii}	2.214 (3)	O2–Ag1–N4	67.38 (9)
Ag1–N4	2.333 (3)	O2–Ag1–O5^{iii}	137.51 (9)
Ag1–O5^{iii}	3.038 (3)	O2–Ag1–C8^{i}	138.86 (10)
Ag1–C8^{i}	3.047 (3)	O2^{i}–Ag1–N3^{ii}	127.51 (11)
Ag1–C8	3.991 (3)	O2^{i}–Ag1–N4	91.07 (11)
C10–O5	3.443 (4)	O2^{i}–Ag1–O5^{iii}	87.59 (10)
C11–O2	3.438 (4)	O2^{i}–Ag1–C8^{i}	22.05 (9)
Ag1–C7	3.159 (4)	Ag1–O2–O5	139.1 (2)
Ag1-C11	3.083 (4)	Ag1–O2–N4	52.53 (9)
Ag1–Ag1^{iii}	5.0247 (5)	Ag1–O2–C8	114.8 (2)
Ag1–Ag1^{ii}	4.2718 (4)	Ag1^{iii}–N3–N4	167.1 (2)

Symmetry codes: (i) −x, −y, 1/2 + z; (ii) ½ − x, 1/2 + y, z − 1/2; (iii) 1/2 − x, 1/2 + y, 1/2 + z

Table 5 Hydrogen bond lengths (Å) and bond angles (°) in the CP **2**

D–H···A	d (D–H)	d (H···A)	d (D···A)	∧ (DHA)
C10–H10···O5	0.960	2.496	3.272	137.89
C11–H11···N4	0.960	2.937	3.543	122.23
C10–H10···N4	0.960	3.055	3.607	117.98
C7–H7···C8	0.961	3.057	3.357	99.83
C11–H11···O5	0.960	3.130	3.442	100.84

by strong hydrogen bonds between the oxygen atoms of the carboxylate group in one chain and the hydrogen atoms of the pyzca ligand in another chain (O5–H10 = 2.496 Å), short contacts (Ag1–O5 = 3.038 Å, Ag1–C8 = 3.991 Å) and π–π stacking (C11–O2 = 3.438 Å, C10–O5 = 3.443 Å) developing two dimensional sheet (Tables 4, 5; Fig. 6). Furthermore, the sheets are also packed mainly through the tetrahedral geometry of the silver atom and by the contacts between the silver atoms and the oxygen atoms of pyzca and the hydrogen bonds and short contacts constructing honey comb 3D-network (Fig. 7). The 4-connections of silver center and pyzca ligands result in a complex 3D topology, with complex helical structure containing nanometer pores (93.47 nm × 174.24 nm) (Figs. 7, 8). The 3D-helical structure of CP **2** exhibits a tetragonal $Ag_5(pyzca)_2$ ring and a chair conformation $Ag_7(pyzca)_6$ ring (Fig. 9). The CP Ag(pyzca), **2′**, was early prepared by self-assembly of pyrazine-2-carboxylate with silver(I) nitrate in the aqueous-acetonitrile solutions [42]. On the comparison, each pyzca ligand in the structure of **2′**, provides three donor sites and connects with three Ag atoms. The 3-connections of silver center with one carboxylate oxygen atom from one pyrazine ligands and two nitrogen atoms from other two pyzca ligands result in a novel 3D topology, which have single helix and triple helices. On the other hand, the silver atom in CP **2** is four connected forming a distorted tetrahedral structure with complex helical structure containing nanometer pores. The 3D-helical structure of CP **2** exhibits a tetragonal ring and a chair conformation ring. In addition the packing structure of CP **2** is further stabilized by hydrogen bonds, short contacts and π–π stacking.

3.3 Infrared Spectra of the CP **1** and **2**

The IR spectra of **1** and **2** exhibit the bands characteristic to qox and pyzca ligands, respectively (Fig. S1). The bands at 3070, 3045 and 759, 626 cm^{-1} are attributed to $\nu_{CH(arom.)}$ and γ_{CH}, respectively of the qox ligand (Table 4). On the other hand, the bands at 1624 and 1553 cm^{-1} are attributed to $\nu_{C=N}$ and $\nu_{C=C}$ of qox ligand in **1**, respectively. In addition, the strong bands at 1301, 1198, 1130 and 1026 cm^{-1} are assigned to the skeletal and C–C vibrations of the qox ligand (Fig. S1). These bands appear at lower wavenumbers than the vibrational frequencies of the free ligand supporting the coordination of qox to the Ag atom and the formation of hydrogen bonds.

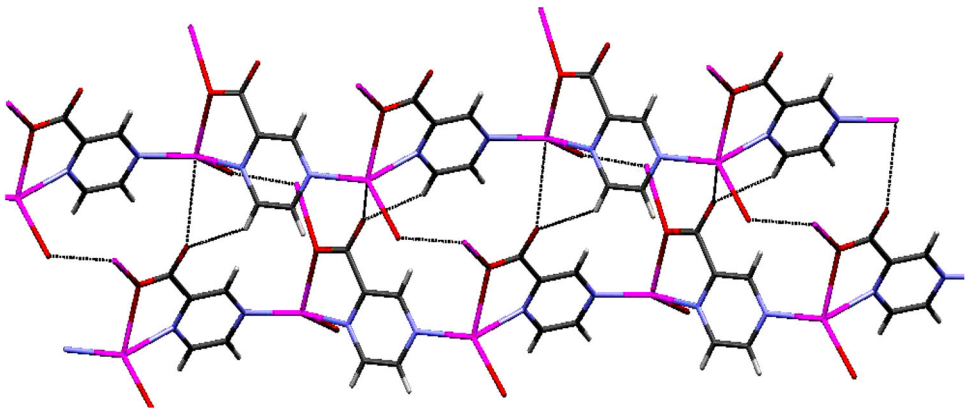

Fig. 6 2D-sheet of the CP **2** via H-bonds and short contacts along the *b* axis

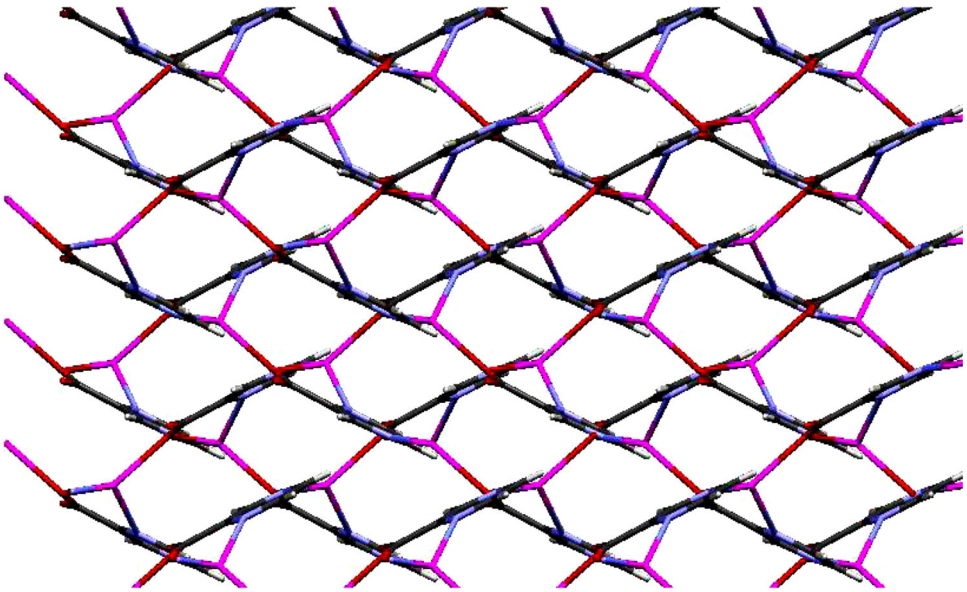

Fig. 7 3D-network honeycomb structure of **2** along the *b* axis

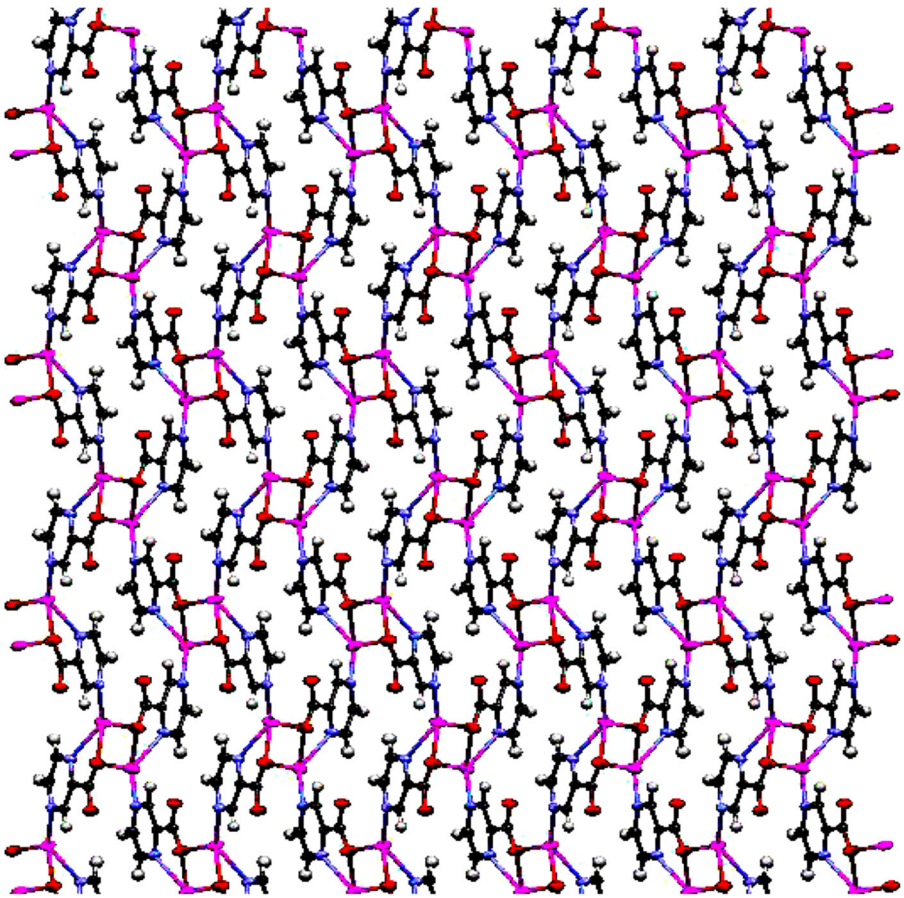

Fig. 8 3D-network helical structure of **2** along the *c* axis

The IR spectrum of **2** reveals also, the characteristic bands of pyzca as compared with those of pyzcaH itself (Table 4; Fig. S1). The IR spectrum of **2** shows, also characteristic strong bands of the carboxylate group at 1520, 1386 cm^{-1} and 721 cm^{-1} corresponding to $\nu_{asy.(COO^-)}$, $\nu_{sym.(COO^-)}$ and $\delta_{(COO^-)}$, respectively. On the other hand, the IR spectrum of **2** shows the bands due to the carbonyl and carbon oxygen stretching vibrations at 1652 and 1255 cm^{-1}, respectively. These bands exhibit shifts to lower wavenumbers than the corresponding vibrational frequencies of the free ligand. The

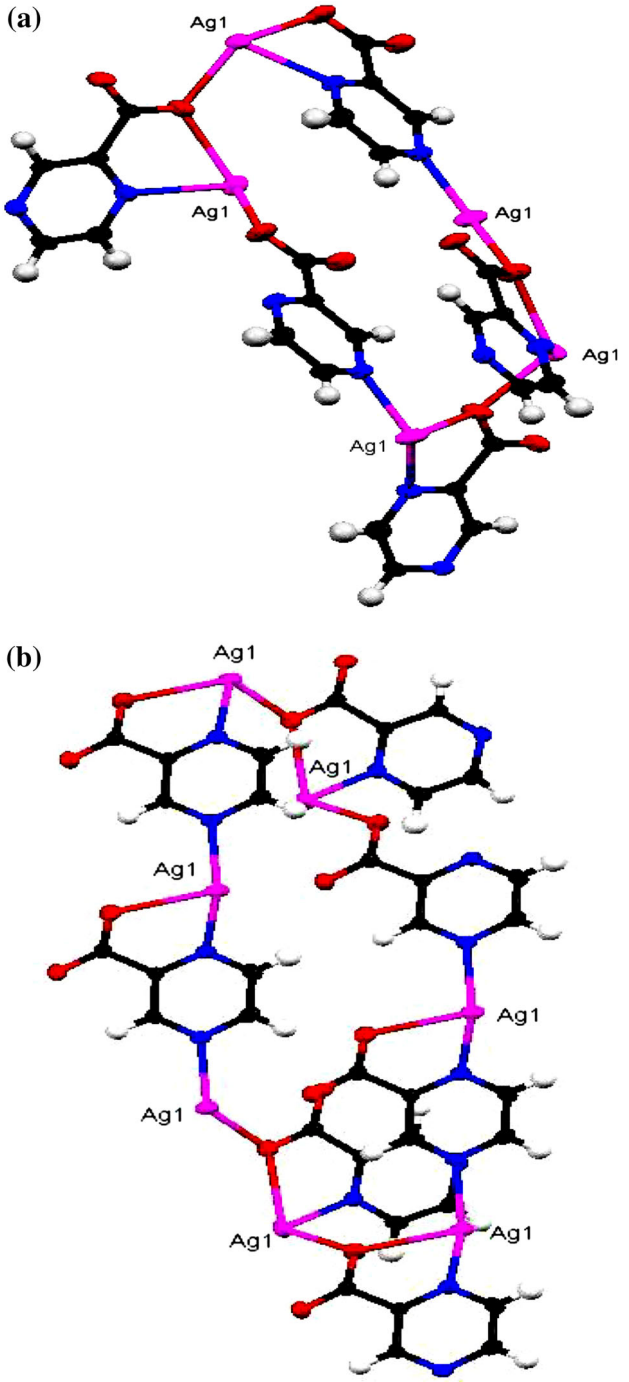

Fig. 9 The tetragonal $Ag_5(pyzca)_2$ ring (**a**) and a chair conformation of $Ag_7(pyzca)_6$ ring (**b**), in **2**

presence of the aromatic systems pyzca in the structure of **2** was confirmed by the display of their characteristic bands. The bands at 3061, 3004 and 787 cm^{-1} are attributed to $\nu_{CH(arom.)}$ and γ_{CH}, respectively of the ligand while the bands at 1625 and 1558 cm^{-1} are attributed to $\nu_{C=N}$ and $\nu_{C=C}$, respectively. These bands appear at more or less the same position as those of pyzcaH itself indicating the coordination of pyzca to the Ag atom and the formation of hydrogen bonds. In addition, the strong bands at 1358, 1168, 1149, and 1053 cm^{-1} are assigned to the skeletal and C–C vibrations of pyzca. The IR spectra of **1**, **2** exhibit weak absorption bands at 531 and 511 cm^{-1}, respectively, due to the Ag–N stretching vibrations which are absent in the spectra of qox and pyzcaH (Table 6).

3.4 Thermogravimetric Analysis

The thermal behavior of **1**, **2** were studied using TGA technique at temperatures up to 800 °C under nitrogen atmosphere by heating rate of 10 °C/min. Thermal gravimetric (TG) of the CP **1** shows that this compound is stable and does not decompose up to 215 °C, (Figs. S2, S3), at which decomposition and pyrolysis of **1** starts. In this stage exothermic removal of the nitrate group occurs in the first step, % Δm % obser. (Calc.) 20.5 (20.6) %. The second step appears at temperature between 220 and 280 °C due to the decomposition of the quinoxaline ligand with a mass loss of 44.1 %, Δm % Calc. 43.8 %. Mass loss calculations show that the final decomposition product is metallic silver, % Δm % obser. (Calc.) 36.5 (36.0) %. On the other hand, the thermogram of **2** exhibits two exothermic steps in the temperature range 300–600 °C corresponding to the decomposition of the complete pyrazine-2-carboxlate ligand, Δm % obser. (Calc.) 52.63 (53.26) %, (Figs. S2, S4). The molecular weight of the residue obtained after complete thermolysis of **2** is coincident with metallic silver (Ag) % Δm % obser. (Calc.) 46.9 (46.67) %. These data indicate the stability of **2** at temperatures up to 300 °C.

3.5 Electronic Absorption and Emission Spectra of the CP **1** and **2**

Before studying the electronic absorption spectrum of **1** and **2**, it is important to consult the spectra of qox and pyzcaH. The electronic absorption spectra of qox and pyzcaH in DMF display three absorption bands at 222–220, 255–275 and 312–320 nm (Table 7). These bands correspond to $^1B_b \leftarrow {}^1A$, $^1L_a \leftarrow {}^1A$ and $^1L_b \leftarrow {}^1A$, respectively [49]. The electronic absorption spectra of **1** and **2** in DMF and in solid state display three absorption bands at 216–222, 253–280, and 310–315 nm (Table 7). The first band is broad and corresponds to $^1B_b \leftarrow {}^1A$ and MLCT transitions while the second one is attributed to the $^1L_a \leftarrow {}^1A$. The last band is due to $^1L_b \leftarrow {}^1A$ transitions. In this case the ^1L_a band suffers a red shift while the ^1L_b band exhibits blue shift under the effect of the coordination to the silver atom.

Table 6 The wavenumbers (cm^{-1}) of different vibrational modes of the CP **1** and **2**

Compound	$\nu_{(CH)}$ (arom)	$\nu_{(C=N)}$ $\nu_{(C=C)}$	$\nu_{(C=O)}$ $\nu_{(C-O)}$	$\nu_{asy.(COO^-)}$ $\nu_{sym.(COO^-)}$ $\delta_{(COO^-)}$	Skeletal and C–C vibrs. of L	δ_{CH} of L	γ_{CH} of L	$\nu_{(Ag-N)}$
qox	3080w	1626m	–	–	1319w–1143m	1428s	788m	–
	3046w	1558w			1069w–1030w		746s	
		1507 s						
[Ag(qox)(NO_3)], **1**	3070w	1624m	–	–	1301m–1198w	1415s	759s	531s
	3045m	1553w			1130m–1026m		626m	
		1501s						
pyzca	3070w	1624sh	1716s	1575s	1330m–1158s	1458s	752s	–
	3004w	1575s	1269m	1394s	1130m–1042s			
				711s				
[Ag(pyzca)], **2**	3061w	1625s	1652s	1520s	1358m–1168s	1406s	787m	511s
	3004w	1558s	1255m	1386m	1149m–1053s			
				721s				

s strong, *m* medium, *w* weak, *sh* shoulder

Table 7 The electronic absorption and emission spectra of the CP **1** and **2**

λ_{abs} (nm)					λ_{em} (nm)		
qox	pyzca	**1**	**2**	Assignment	**1**	**2**	Assignment
222	220	216	222	$^1B_b \leftarrow {}^1A$	355	365	Close lying π–π* transition
255	275	253	280	$^1L_a \leftarrow {}^1A$	425	430	Lowest π–π* state
312	320	310	315	$^1L_b \leftarrow {}^1A$			

The emission spectra of **1** and **2** should resemble those of qox and pyzcaH. The emission spectra of qox and pyzcaH in DMF display well developed peak at 355and 365 nm, one shoulder at 425 and 430 nm, respectively (Table 7; Fig. 10). These two structured bands correspond to the close lying π–π* transitions [13, 35, 50–52]. The emission spectra of **1** and **2** show a broad band at wavelengths 355–430 nm (Table 7; Fig. 10). The main band at 355 and 365 nm in the emission spectra of **1** and **2**, respectively exhibits blue shift than that of qox and pyzcaH by about 55–50 nm moving from the visible to the UV region. Thus, the luminescence behavior of qox and pyzcaH show excellent sensitivity towards silver which makes it attractive as luminescent sensor.

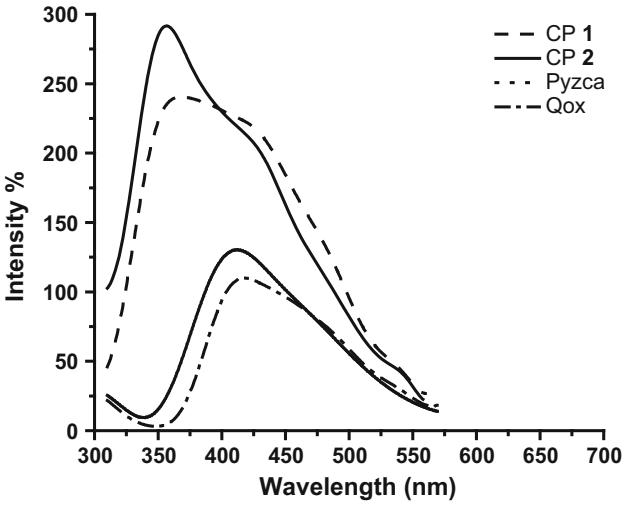

Fig. 10 Emission spectra of the free ligands and the CP **1** and **2** (solid states) ($\lambda_{ex} = 300$ nm)

4 Conclusions

This work presents two Ag(I) CP generated from the quinoxaline and pyrazinecarboxyate. The crystal structures of **1** and **2** display 1D-extended chain of $[Ag(qox)]_n$ and $[Ag(pyzca)]_n$, respectively. Self-assembly of **1** by coordination bonds, hydrogen bonds, π–π stacking and short contacts grow the structure to a three dimensional network creating wide channels to accommodate the coordinated nitrate ions. On the other hand, the versatility of the carboxylate ligand in pyzca and the 4-connections of silver center result in a complex 3D-helical topology that contains nanometer sized voids. The overall packing arrangement of 2 is further stabilized by hydrogen bonds, π–π stacking and short contacts. The emission spectra of **1** and **2** exhibit blue shift than those of qox and pyzcaH. Thus, the luminescence behaviors of qox and pyzcaH show excellent sensitivity towards silver which makes it attractive as luminescent sensor.

5 Supplementary Data

CCDC 1027163-1027164 contain the supplementary crystallographic data for **1**, **2**. These data can be obtained free of charge via http://www.ccdc.cam.ac.uk/conts/retrieving.html, or from the Cambridge Crystallographic Data Centre, 12 Union Road, Cambridge CB2 1EZ, UK; fax: (+44) 1223-336-033; or e-mail: deposit@ccdc.cam.ac.uk.

References

1. L.E. Kreno, K. Leong, O.K. Farha, M. Allendorf, R.P. Van Duyne, J.T. Hupp, Chem. Rev. **112**, 1105–1125 (2012)
2. D. Maspoch, D. Ruiz-Molina, J. Veciana, Chem. Soc. Rev. **360**, 770–818 (2007)
3. W. Lin, Z. Wang, L. Ma, J. Am. Chem. Soc. **121**, 11249–11250 (1999)
4. U. Mueller, M. Schubert, F. Teich, H. Puetter, K. Schierle-Arndt, J. Pastre, J. Mater. Chem. **16**, 626–636 (2006)
5. J.L.C. Rowsell, E.C. Spencer, J. Eckert, J.A.K. Howard, O.M. Yaghi, Science **309**, 1350–1354 (2005)
6. D. Bradshaw, J.B. Claridge, E.J. Cussen, T.J. Prior, M.J. Rosseinsky, Acc. Chem. Res. **38**, 27–282 (2005)
7. M.D. Allendorf, C.A. Bauer, R.K. Bhakta, R.J.T. Houk, Chem. Soc. Rev. **38**, 1330–1352 (2009)
8. C.-Y. Su, C.-L. Chen, J.-Y. Zhang, B.-S. Kang, Silver(I) coordination polymers, in *Design and Construction of Coordination Polymers*, ed. by M.-C. Hong, L. Chen (Wiley, Hoboken, 2009)
9. S.E.H. Etaiw, M.M. El-bendary, J. Inorg. Organomet. Polym. **23**, 510–518 (2013)
10. S.E.H. Etaiw, A.S. Sultan, M.M. El-bendary, J. Organomet. Chem. **696**, 1668–1676 (2011)
11. S.E.H. Etaiw, A.S. Badr El-din, M.M. El-bendary, Z. Anorg. Allg. Chem. **639**, 810–816 (2013)
12. S.E.H. Etaiw, M.M. El-bendary, Spectrochim. Acta A **110**, 304–310 (2013)
13. S.E.H. Etaiw, A.S. Fouda, S.N. Abdou, M.M. El-bendary, Corros. Sci. **53**, 3057–3665 (2011)
14. S.E.H. Etaiw, M.M. El-bendary, App. Catal. B **126**, 326–333 (2012)
15. S. Kitagawa, R. Matsuda, Coord. Chem. Rev. **251**, 2490–2509 (2007)
16. Y.B. Dong, X. Zhao, B. Tang, H.Y. Wang, R.Q. Huang, M.D. Smith, H.C. Zur Loye, Chem. Commun., 220–221 (2004)
17. Y.B. Dong, X. Zhao, R.Q. Huang, Inorg. Chem. **43**, 5603–5612 (2004)
18. M. Pascu, F. Tuna, E. Kolodziejczyk, G.I. Pascu, G. Clarkson, M.J. Hannon, Dalton Trans., 1546–1555 (2004)
19. D.Y. Wu, W. Huang, C.Y. Duan, Q.J. Meng, Inorg. Chem. Commun. **10**, 1009–1013 (2007)
20. Y.B. Dong, H.Q. Zhang, J.P. Ma, R.Q. Huang, Cryst. Growth Des. **5**, 1857–1866 (2005)
21. Y. Bai, C.Y. Duan, P. Cai, D.B. Dang, Q.J. Meng, Dalton Trans., 2678–2680 (2005)
22. Q.Z. Sun, M.L. Wei, Y. Bai, C. He, Q.J. Meng, C.Y. Duan, Dalton Trans., 4089–4094 (2007)
23. C.M.R. Juan, B. Lee, Coord. Chem. Rev. **183**, 43–80 (1999)
24. T.N. Guru Row, Coord. Chem. Rev. **183**, 81–100 (1999)
25. I. Unamuno, J.M. Gutiérrez-Zorrilla, A. Luque, P. Román, L. Lezama, R. Calvo, T. Rojo, Inorg. Chem. **37**, 6452–6460 (1998)
26. M.W. Hosseini, Acc. Chem. Res. **38**, 313–323 (2005)
27. K. Chainok, S.M. Neville, C.M. Forsyth, W.J. Gee, K.S. Murray, S.R. Batten, CrystEngComm **14**, 3717–3726 (2012)
28. P.J. Steel, C.M. Fitchett, Coord. Chem. Rev. **252**, 990–1006 (2008)
29. Q. Chu, D.C. Swenson, L.R. MacGillivray, Angew. Chem. **117**, 3635–3638 (2005)
30. R. Santra, K. Biradha, Cryst. Growth Des. **10**, 3315–3320 (2010)
31. O.-S. Jung, Y.J. Kim, Y.-A. Lee, S.W. Kang, S.N. Choi, Cryst. Growth Des. **4**, 23–24 (2004)
32. P.-P. Zhang, J. Peng, H.-J. Pang, J.-Q. Sha, M. Zhu, D.-D. Wang, M.-G. Liu, Z.-M. Su, Cryst. Growth Des. **11**, 2736–2742 (2011)
33. P.-S. Cheng, S. Marivel, S.-Q. Zang, G.-G. Gao, T.C. Mak, Cryst. Growth Des. **12**, 4519–4529 (2012)
34. R.-W. Huang, Y. Zhu, S.-Q. Zang, M.-L. Zhang, Inorg. Chem. Commun. **33**, 38–42 (2013)
35. D. Sun, G.-G. Luo, N. Zhang, Q.-J. Xu, C.-F. Yang, Z.-H. Wei, Y.-C. Jin, L.-R. Lin, R.-B. Huang, L.-S. Zheng, Inorg. Chem. Commun. **13**, 290–293 (2010)
36. V.T. Yilmaz, E. Senel, E. Guney, C. Kazak, Inorg. Chem. Commun. **11**, 1330–1333 (2008)
37. E. Soyer, F. Yilmaz, V.T. Yilmaz, O. Buyukgungor, W.T. Harrison, J. Inorg. Organomet. Polym Mater. **20**, 320–325 (2010)
38. L. Brammer, M.D. Burgard, M.D. Eddleston, C.S. Rodger, N.P. Rath, H. Adams, CrystEngComm **4**, 239–248 (2002)
39. M.A.M. Abu-Youssef, V. Langer, L. Öhrstrom, Dalton Trans., 2542–2550 (2006)
40. H.-Y. Liu, H. Wu, J.-F. Ma, J. Yang, Y.-Y. Liu, Dalton Trans., 7957–7968 (2009)
41. H.-Y. Liu, H. Wu, J.-F. Ma, S.-Y. Song, J. Yang, Y.-Y. Liu, Z.-M. Su, Inorg. Chem. **46**, 7299–7311 (2007)
42. S. Qin, S. Lu, Y. Ke, J. Li, X. Wu, W. Du, Solid State Sci. **6**, 753–755 (2004)
43. Z.-H. Wang, D.-F. Wang, T. Zhang, R.-B. Huang, L.-S. Zheng, J. Mol. Struct. **1064**, 27–31 (2014)
44. M. Park, J. Jang, S.Y. Moon, O.-S. Jung, J. Mol. Struct. **1062**, 89–95 (2014)
45. S.E.H. Etaiw, D.M. Abd El-Aziz, A.S. Badr El-din, Polyhedron **28**, 873–882 (2009)
46. S.E.H. Etaiw, M.M. El-bendary, J. Coord. Chem. **63**, 1038–1051 (2010)
47. S.E.H. Etaiw, A.S. Sultan, A.S. Badr El-din, Eur. J. Med. Chem. **46**, 5370–5378 (2011)
48. S.E.H. Etaiw, A.S. Badr El-din, J. Inorg. Organomet. Polym. **21**, 1–8 (2011)
49. H.H. Jaffe, M. Orchin, *Theory and Applications of Ultraviolet Spectroscopy*, 5th edn. (Wiley, New York, 1970)
50. S.E.H. Etaiw, A.S. Badr El-din, J. Inorg. Organomet. Polym. **21**, 110–117 (2011)
51. S.E.H. Etaiw, S.N. Abdou, J. Inorg. Organomet. Polym. **23**, 1296–1304 (2013)
52. F.-F. Li, J.-F. Ma, S.Y. Song, J. Yang, Y.-Y. Liu, Z.-M. Su, Inorg. Chem. **44**, 9374–9383 (2005)